Please cite this paper as:

Peris-Sayol, G., Paya-Zaforteza, I., Alos-Moya, J., Hospitaler, A. Analysis of the influence of geometric, modeling and environmental parameters on the fire response of steel bridges subjected to realistic fire scenarios.Computers and Structures 2015,158:333-345.

DOI: 10.1016/j.compstruc.2015.06.003

Analysis of the influence of geometric, modeling and environmental parameters on the fire response of steel bridges subjected to realistic fire scenarios

G. Peris-Sayol, I. Paya-Zaforteza*, J. Alos-Moya, A. Hospitaler

[1]*ICITECH, Departamento de Ingeniería de la Construcción, Universitat Politècnica de València. Camino de Vera s/n, 46022 Valencia, Spain*

Authors e-mail addresses:
Guillem Peris-Sayol: guipesa2@upv.es
Ignacio Paya-Zaforteza: igpaza@ cst.upv.es
Jose Alos-Moya: joalmo11@upv.es
Antonio Hospitaler: ahospitaler@cst.upv.es

Abstract

This paper studies bridge fires by using numerical models to analyze the response of a typical girder bridge to tanker truck fires. It explains the influence of fire position, bridge configuration (vertical clearance, number of spans) and wind speed on the bridge response. Results show that the most damage is caused by tanker fires close to the abutments in single span bridges with minimum vertical clearance and under windless conditions. The paper provides new insights into modeling techniques and proves that bridge response can be predicted by FE models of the most exposed girder, which saves significant modeling and analysis times.

Keywords: fire, Computational Fluid Dynamics, steel girder bridge, parametric study, performance-based design.

* Corresponding author. Tel: +34 963877562; fax: +34 963877568

1. Introduction

The loss of a critical component, such as a bridge, from a transportation system can have serious social and economic consequences (e.g. Chang and Nojima [1], Zhu et al. [2]). Bridge engineering should therefore pay a lot of attention to designing for accidental load events, such as earthquakes, winds or ship collisions (see e.g. Ghosn et al. [3] and Cheng [4]). Recent studies also show that bridge fires are another major hazard. Mostafaei and McCartney [5], Wright et al. [6] pointed out that more than 500 fatal crashes happened on bridges in the last fourteen years across the US and Canada. These events had large direct costs (related to repairs and reconstruction work) and indirect costs (traffic delays from bridge closures and rebuilding). For example, the collapse of two spans of the MacArthur Maze in Oakland, USA on April 29th 2007 due to a fire gave rise to repairs and rebuilding operations costing more than US $9m [7]. In addition, the closure of the Maze was estimated to have a total economic impact of US $6 million a day on the San Francisco Bay Area [8]. Another example is provided by the bridge fire caused by a tanker truck that crashed on the Interstate 81 Highway near Harrisburg (PA, USA) on May 9th 2013. This fire forced the closure of one highway exit and resulted in region-wide traffic disruptions. Repair work took seven months at a direct cost of more than $13 m [9].

Recent reviews of the literature (Garlock et al. [10], Mostafaei et al. [11]) show that, despite their importance, bridge fires have received very little attention from research groups. In fact, fire safety engineering and structural fire engineering have mainly been concerned with building and tunnel fires (see e.g. Jiang and Usmani [12], Couto et al. [13], Quiel et al. [14], Moura Correia et al. [15], Moliner et al.[16], Xi et al [17], Elhami et al. [18], Wang et al. [19], Maraveas and Brakas [20]). However, bridge fires have special characteristics and deserve a particular approach. This can be due to several reasons, such as the cause of the fire, fire loads, fire ventilation conditions, the use of fire protection measures, and the type of connections between structural members (see Payá-Zaforteza and Garlock [21] for further information).

Within this general context, this paper carries out a comprehensive parametric study of the fire response of a typical steel girder bridge subjected to real fire scenarios. The analyses use numerical models to study the influence of the position of the fire, the geometry of the bridge (type of bridge substructure and vertical clearance), and the magnitude of the wind loads in the bridge's response to the fire. The study also addresses important numerical issues, such as the modeling of the bridge deck bearings and the bridge deck elements that should be included in the models. A method based on computational fluid dynamics (CFD) was used for the fire models and finite elements were used to obtain the

bridge's thermo-mechanical response. This method was validated by Alós-Moya et al. [22] with data collected from an actual case of bridge failure. We consider the analyses presented here to be of great importance since: (a) steel girder bridges are widely used [23] and are especially vulnerable to fire events [10], (b) research on bridge fires is scarce and is based more on the use of standard fires or predefined fire events than on the analysis of realistic fire scenarios, and (c) the paper proposes new modelling techniques and enables a qualitative and quantitative understanding of the factors that influence the fire response of a bridge. This study complements previous works (see e.g. Wright et al. [6], Payá-Zaforteza and Garlock [21], Aziz et al. [24], Quiel et al. [25],Gong and Agrawal [26]) and paves the way for easier identification of critical bridges with respect to fire risks, as well as for the wider application of numerical models to improve bridge fire response and bridge resilience.

2. Case study and parameters analyzed

The prototype bridge used in the present study is a simply supported bridge designed by the Federal Highway Administration (FHWA) of the United States of America. The bridge spans 12.2 m and its vertical clearance is 5 m. Its cross section and plan view are shown in Fig. 1. The bridge consists of five hot rolled type W33x141 steel girders. The beams support a 0.2 m thick reinforced concrete slab but the slab is not connected to the girders and, therefore, there is no composite action. This was a common design decision for bridges with span lengths smaller than 15 m at the time when the bridge was designed (Xanthakos [27]). Transverse diaphragms are placed at mid span and at the supports to laterally stiffen the bridge deck. The bridge has two expansion joints at its extremities with a width of 3.6 cm. At ambient temperature, material properties are those of the nominal values for A36 steel, which means its minimum yield stress is 250 MPa. The response of one of the bridge girders to the hydrocarbon fire was previously analyzed by Payá-Zaforteza and Garlock in [21]. This paper delves further into this case and studies the influence of several parameters on the response of the bridge to realistic fire scenarios after a tanker truck accident, including the following parameters:

- Position of the fire load (see Section 3).
- Structural boundary conditions (see Section 5.1).
- Elements included in the thermo-mechanical finite element model, i.e., analyzing only one girder versus the entire bridge (see Section 5.2).
- Bridge vertical clearance (see Section 5.3).
- General configuration of the bridge: single span versus three-span bridge (see Section 5.4).
- Wind action during the fire event (see Section 5.5).

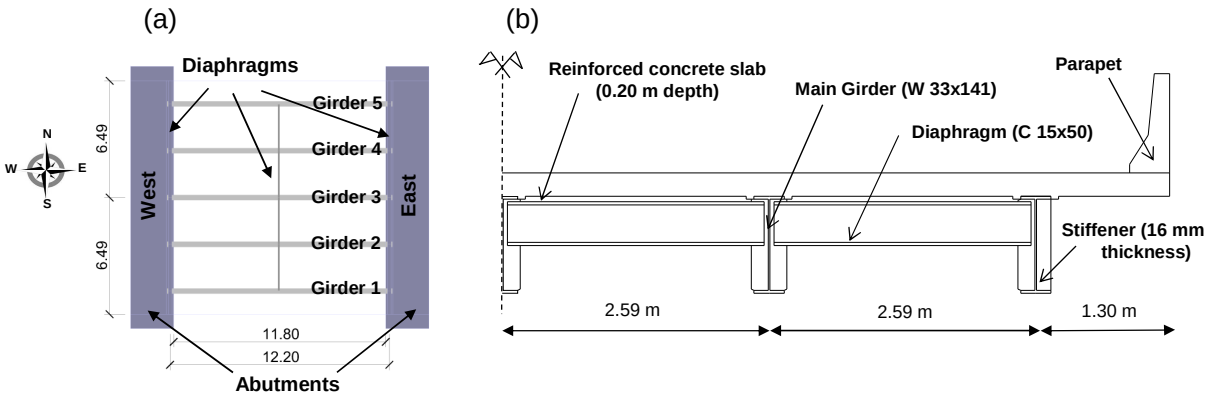

Fig. 1. Bridge definition. (a) Plan view (without the concrete slab), (b) half section.

All the analyses are carried out following a three-step numerical approach. In the first step a model of a fire scenario is built with FDS computer fluid dynamics software [28]. The temperatures in the most fire-exposed girder in the bridge or in the full bridge are obtained through a thermal analysis by Abaqus software [29]. Finally, the structural response of the bridge is obtained on Abaqus [29] considering both non-linearities (geometrical and mechanical) as well as temperature-dependent material properties.

3. Computational Fluid Dynamics model

Two fire models of hypothetical fire events were developed with FDS software [28]. FDS uses Computational Fluid Dynamics (CFD) techniques and contains large eddy simulation (LES) turbulence models. It is used to predict in a control volume engineering variables such as temperatures, heat fluxes or gas pressures involved in the event. FDS was developed at the National Institute of Standards and Technology (NIST) in the USA and has gone through an extensive validation program [30]. The use of FDS to study bridge fires was validated by Alos-Moya et al. [22] using FDS and Abaqus to analyze an overpass failure caused by a tanker fire.

Building the FDS model requires defining: (1) a control volume with its boundary conditions representing the volume in which the entire analysis is carried out, (2) a geometry included in the control volume which represents the geometry of the case study, (3) A mesh or discretization of the control volume, (4) material properties (conductivity, density, specific heat and emissivity), (5) fire sources, (6) a combustion model, and (7) sensors or elements of the model where the outputs (e.g. temperatures) are recorded. The components of the FDS model are described below.

3.1 Control volume and mesh

The control volume used in this study includes the bridge as well as part of its approaches. It measures 43.92 m. x 30.82 m. x 10.20 m. along the *x*, *y* and z-directions respectively. The volume has a total of 1,658,880 parallelepiped cells and all the cells have dimensions of 0.20 m x 0.19 m x 0.21 m. This control volume and mesh size were the result of a sensitivity analysis and are a trade-off between precision and calculation times. It is important to note that the FDS mesh size does not coincide with the mesh used in the thermo-mechanical models built with Abaqus. Therefore, the authors developed a procedure to transfer the FDS results to Abaqus. This procedure is described in Section 4.4.

3.2 Fire Load and combustion model

Previous studies (see Wright et al. [6], Garlock et al. [21], Alós-Moya et al. [22], and Peris-Sayol et al. [31]), showed that an accident involving a tanker truck carrying gasoline under a bridge was the worst possible scenario when analyzing the fire response of bridge decks made of steel I-girders. The fire load used in this paper is thus related to this type of vehicle. The tanker truck is modeled as a horizontal surface of 30 m^2 (12 x 2.5m) at one meter above the road level. The heat release rate per unit area (HRRPUA) curve increases linearly from 0 to a maximum value $HRRPUA_{MAX}$ in 30 s and remains constant until failure. $HRRPUA_{MAX}$ was taken as 2400 kW/m^2 which is the HRR of a gasoline pool fire with a diameter exceeding 3 m [32]. The HRRPUA curve does not have a decay phase, as the numerical models developed simulate fires with a maximum duration of one hour and after that time only 30% of the available fire load had been consumed.

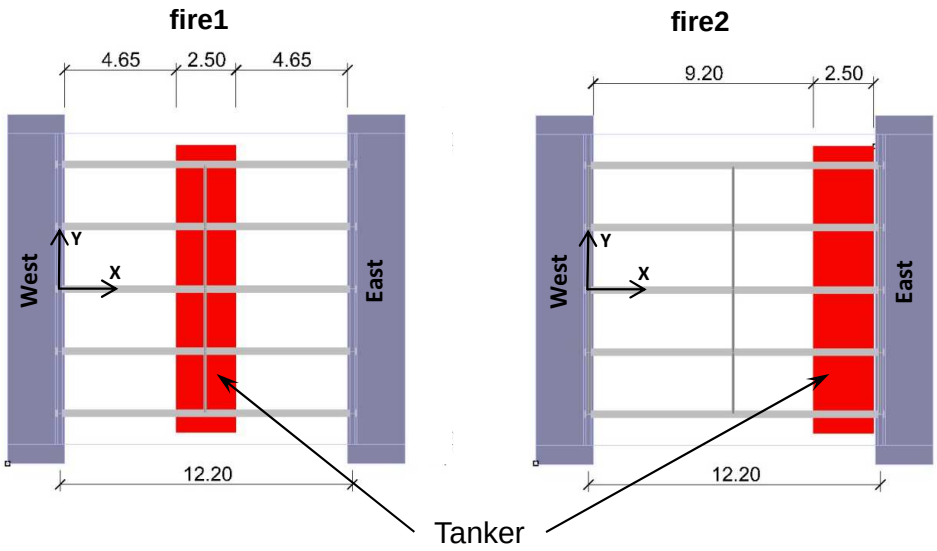

Fig. 2. Fire scenarios considered.

Two fire scenarios related to the position of the tanker fire were considered (see Fig. 2). One was of a tanker truck located under the central girder of the bridge (Girder 3) at the bridge mid-span (scenario called “fire1” henceforth) and the other was close to the east abutment (scenario called “fire2” henceforth). The fire models used the mixture fraction combustion model proposed by FDS [28] and a LES turbulence model with a Smagorinsky coefficient equal to 0.2.

3.3 Adiabatic temperatures

The adiabatic surface temperature developed by Wickström et al. [33] is used to transfer the information obtained by the fire model to the thermal model. This adiabatic surface temperature is a fictitious temperature obtained by FDS assuming that the structural element is a perfect insulator and is commonly used for calculating both convective and radiative heat transfer. It is an expression of the heat flux as a gas temperature which enables the fire model results to be easily introduced into the thermo-mechanical model. Adiabatic temperatures are measured in FDS with sensors whose location is defined by the user. The model includes 465 sensors to measure the adiabatic temperatures in 155 cross-sections of the bridge (31 sections per girder). Note that each cross section was monitored with three sensors located on the bottom face (Sensor 0), the south face (Sensor 1) and the north face (Sensor 2) of each girder (see Fig. 3), as preliminary analyses had shown that this sensor distribution accurately captured the temperature distribution along the girders.

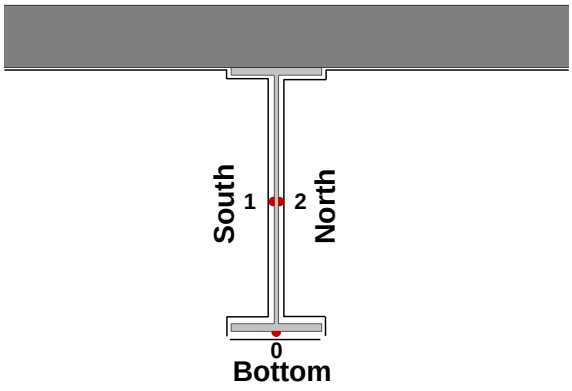

Fig. 3. FDS model. Adiabatic surface temperature sensors in a typical monitored cross section.

Fig. 4 displays FDS results for the “fire1” scenario in the steady state of the fire event, when the fire had completely developed. Fig. 4a shows a 3D view of the bridge and its surroundings. Figs. 4b and 4c plot the adiabatic temperatures on the bottom face of all the bridge girders and on all the faces of the most exposed girder (Girder 3). As the tanker is under the bridge at the center, Girder 3 has the highest temperatures. Web temperatures are higher than bottom flange temperatures due to radiation effects and reach maximum values

(close to 1300 ºC) in the area of Girder 3 immediately above the burning tanker. Temperatures vary longitudinally between 1250 ºC and 950 ºC in Girder 3, between 1200 ºC and 900 ºC in Girders 2 and 4 and between 950 ºC and 450 ºC in Girders 1 and 5 (450 ºC is reached on the surfaces of the web girders not directly exposed to the fire). When the "fire2" scenario is analyzed, the temperatures in Girder 3 vary between 1300 and 1000 ºC and the maximum temperatures are obtained in the section of Girder 3 closest to the East abutment. It is noticeable that in the "fire2" scenario maximum temperatures are higher than in "fire1", because of heat accumulation near the abutments.

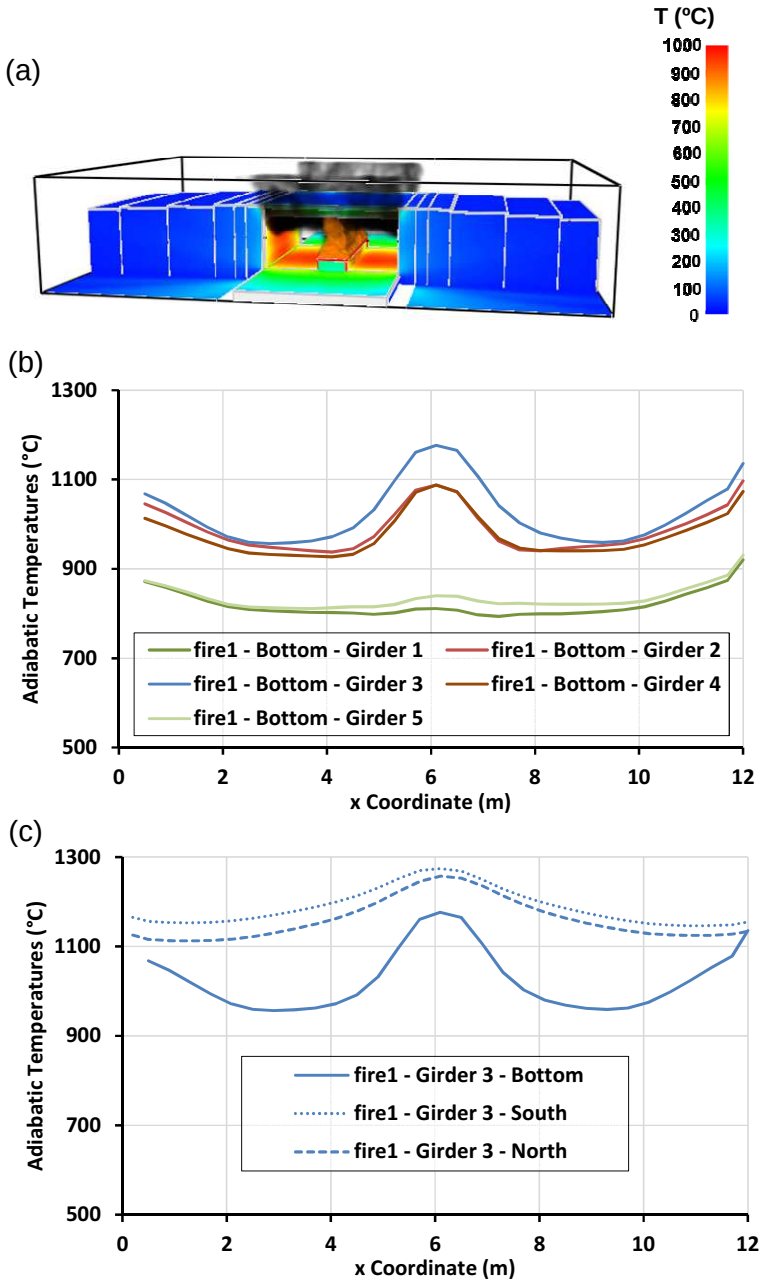

Fig. 4. FDS results for the "fire1" scenario in the steady state: (a) 3D view of the bridge, (b) Adiabatic temperatures on the bottom flange of each girder, (c) Adiabatic temperatures on all faces of Girder 3.

4. Finite element model for thermo-mechanical analysis

The thermo-mechanical response of the bridge is obtained with Abaqus finite element software in two steps. In the first step, a thermal analysis is carried out using the adiabatic surface temperatures given by FDS as an input. The heat transfer analysis provides the transient nodal temperatures with respect to time as an output. In the second step, the transient nodal temperatures are read from the thermal analysis and the corresponding temperature-dependent mechanical material properties are used to find the equilibrium of the structure. Note that in the first step the concrete slab is included in the model and the analysis, while in the second step the slab influence is neglected, since the bridge is not a composite bridge, although appropriate boundary conditions are considered to take into account the influence of the slab. The FE modeling is explained in detail below.

4.1 Mesh

Figs. 5a and 5b show the mesh used for the thermal and mechanical analyses. Note that, as will be explained in detail in Section 5, some of the FE models include the full bridge and some include a single girder, however the mesh of each girder is the same in both types of model. The thermal models used Abaqus DC3D8 elements, while Abaqus C3D8 elements were used for the mechanical analyses. The first element has 8 nodes with one degree of freedom in each node, while the second element has 8 nodes and 3 degrees of freedom in each node. The FE structural analyses include geometric and material non-linearity. The use of 3D elements is motivated by the need to capture local phenomena such as web buckling. As can be seen in Fig. 5, the mesh is finer at mid-span and near the supports, as these are areas of high stress where stiffeners are placed. The FE models of a single girder contain 21,717 nodes and 14,884 finite elements in the thermal analysis and 18,183 nodes and 12,624 elements in the mechanical analysis. The FE models of the full bridge contain 122,949 nodes and 83,060 finite elements in thermal analysis and 105,279 nodes and 71,760 elements in the mechanical analysis. Note that there are fewer elements in the mechanical FE models as they do not include the concrete slab. Note also that models with solid elements were used in this research because: (a) calculation times were affordable, (b) previous research (Alós-Moya et al., [22]) showed that they could accurately estimate the response of a bridge to a fire, and (c) previous studies (Wright et al. [6], Peris-Sayol et al. [34]) showed that they had a better performance than models using exclusively shell elements.

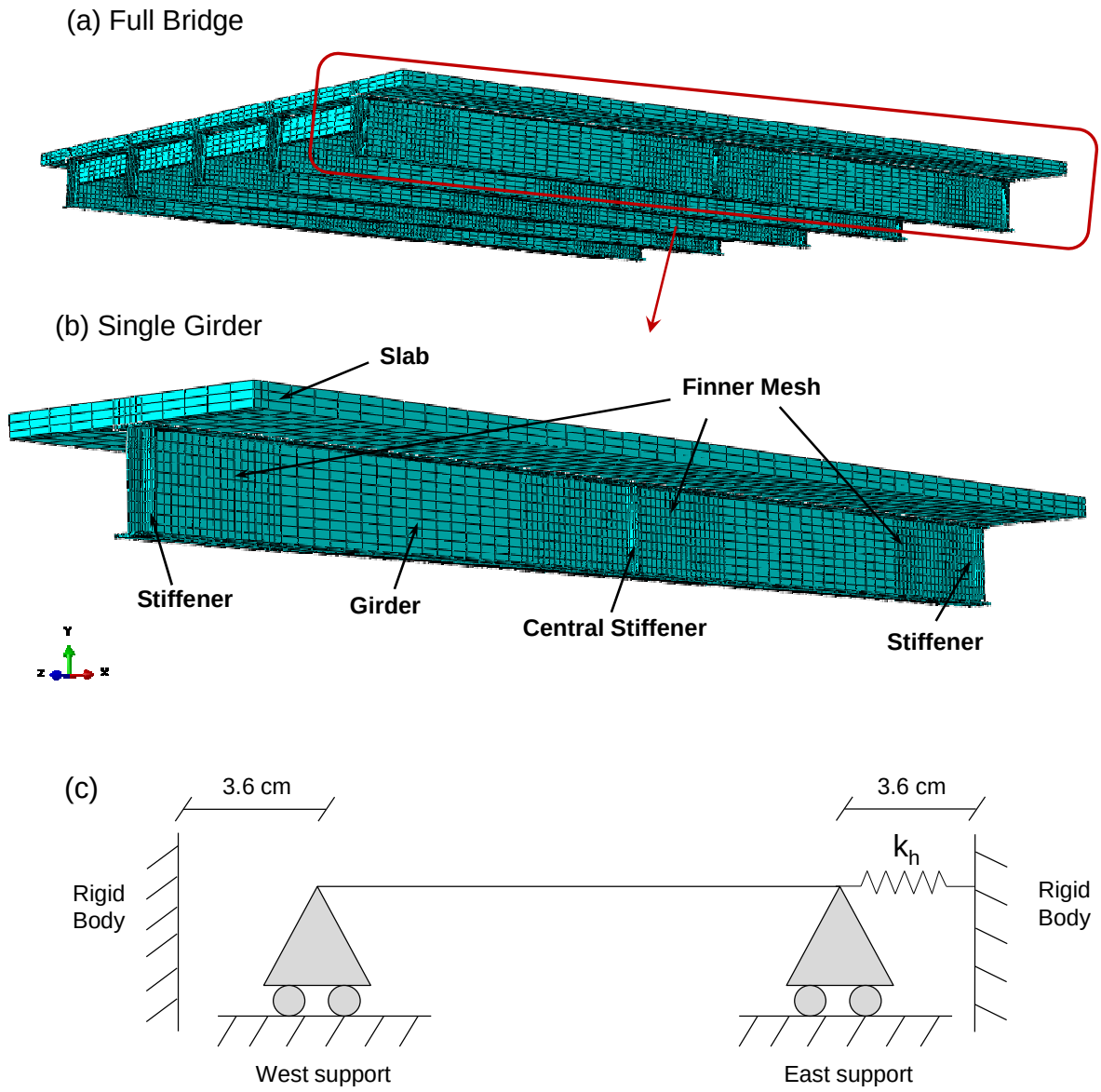

Fig. 5. FE model and mesh: (a) Full bridge, (b) Single girder, (c) Schematic boundary conditions.

4.2 Material Properties

The thermal and mechanical properties of the steel and concrete materials in the bridge were taken from Eurocode 2 [35] and 3 [36]. The steel used is A36, with a yielding limit of 250 MPa and the strain hardening proposed in Eurocode 3. Engineering values of stresses (σ) and strains (ε) were converted into true stress strain laws (σ_n-ε_n) and entered in Abaqus. Only the concrete thermal properties were characterized in the heat transfer model (density, specific heat and conductivity) assuming that calcareous aggregates where used to make the concrete. The upper limit of concrete thermal conductivity proposed in Eurocode 2 [35] was used.

4.3 Boundary conditions

The bridge studied is a single span, simply-supported bridge in which the East support is pinned and the West support is a roller. The restrictions of both supports in the model are applied on a surface that represents the support. This surface is located on the bottom face of the bottom flange just below the stiffener. The length of this surface is 46 mm and its width is 293 mm (girder width). These restraints are represented in Fig. 5c and detailed below.

As explained by Paya-Zaforteza and Garlock [21] the maximum thermal expansion of a bridge in a fire must be limited, as the bridge girders cannot expand indefinitely due to the existence of an adjacent abutment and/or span. Therefore, the maximum longitudinal displacement of the roller bridge supports is the expansion joint width (equal to 3.6 cm in the case study analyzed in this paper). In addition, a previous study by Peris-Sayol et al. [37] showed that when the sections of the bridge deck supported by a roller come into contact with an adjacent abutment or span, thermal expansion is restrained and very high horizontal reaction forces appear in the pinned support. In these conditions, the pinned support might fail to restrain the longitudinal movement of the bridge and would become a horizontal spring. Peris-Sayol et al. [37] performed a parametric study of the stiffness of the horizontal spring (k_h) and concluded that two values of the spring constant (k_h close to *0* and $k_h=\infty$, the latter case representing a pinned support) are enough to capture the response of the bridge. Both values of k_h are considered in the numerical models presented in this paper and their influence on the results is discussed in Section 5.1. In any case, a rigid body was created in the FE structural models with Abaqus R3D4 rigid elements at a distance from the East and West outer cross sections of the bridge equal to the expansion joint width. In doing so, the axial expansion of the nodes of the outer cross sections of the bridge is restrained once their horizontal displacement equals the width of the expansion joint. Other boundary conditions are:

- The restraint imposed by the transverse diaphragms of the bridge in the models that include a single girder is considered by preventing the transverse displacement of the beam in the diaphragm-stiffener contact area.

- The influence of the concrete slab in the mechanical models is considered by preventing the transverse displacement of the upper face of the top flange.

4.4 Discretization of the temperatures along the length of the girders.

As has been explained in Section 3, FDS obtains the adiabatic surface temperatures in selected nodes of the CFD model. The specific values of these temperatures depend on the

girder considered and, for each girder, vary along the axis of the bridge and also within the girder cross section, as explained in Section 3.3. To transform FDS results to Abaqus inputs, the curves describing the adiabatic temperatures were transformed into stepped curves, as shown in Fig. 6a. Each stepped curve has 16 steps, the temperature at each step being the average of all the temperatures measured by FDS in the step and zone (see Fig. 6b). Abaqus heat transfer models use a heat transfer coefficient (h_c) of 35 W/m^{2}K and an emissivity coefficient (ε) of 0.7 for a gasoline fire, according to EC-1 [38] and EC-3 [36].

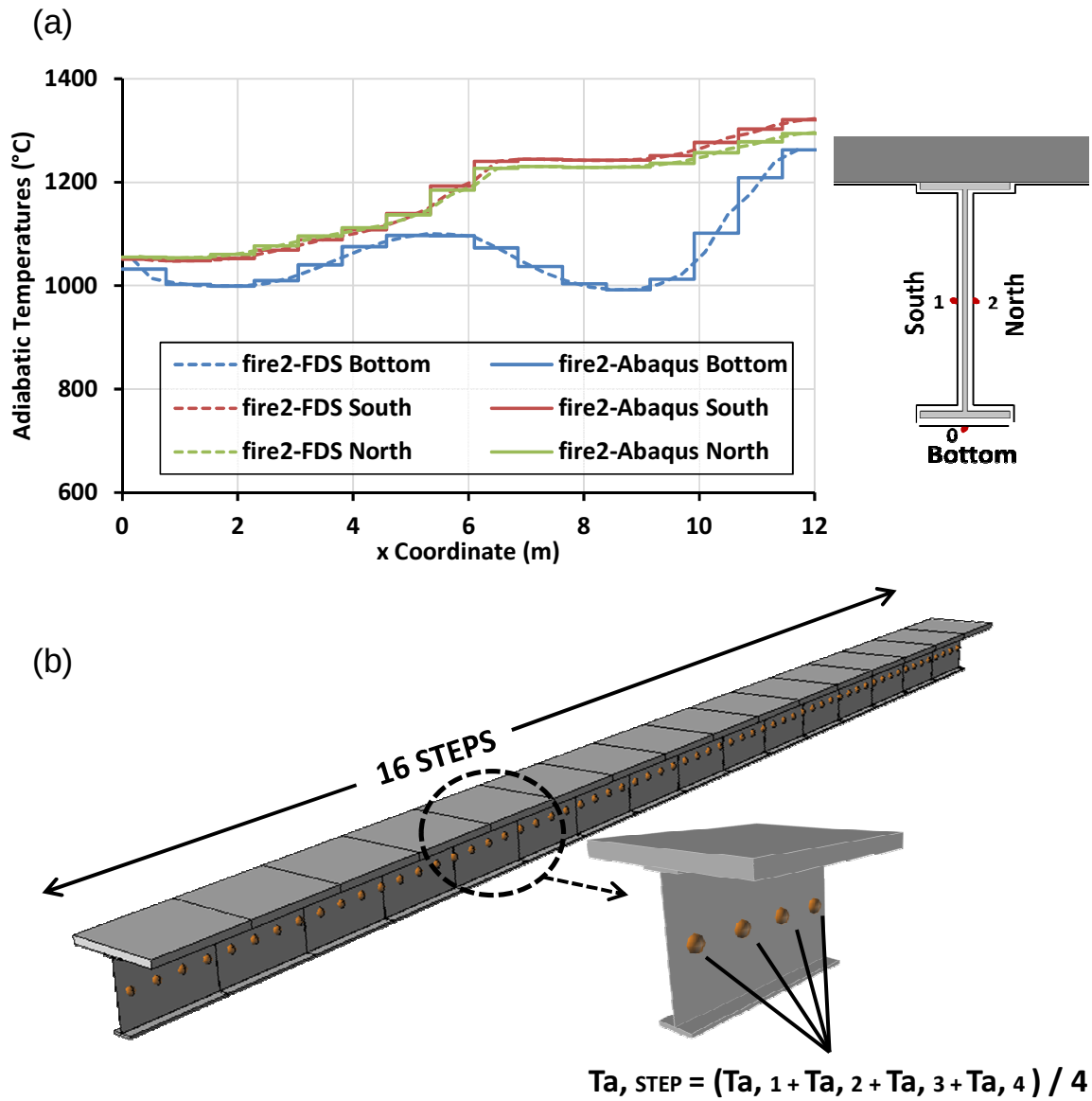

Fig. 6. (a) Girder 3. Example of 16-step discretization of the adiabatic temperature curves for merging CFD with Abaqus. (b) Model showing the 16 steps and the calculation of the average temperature at each step.

4.5 Gravity Loads

The following gravity loads were considered:

(a) The self-weight of the steel girders and their stiffeners is considered by Abaqus automatically from their dimensions, assuming a steel density of 7850 kg/m^3.

(b) A surface load of 43.4 kN/m^2 is applied to the upper surface of the upper flange to simulate the self-weight of the concrete slab.

(c) For the for the weight of the pavement, a surface load of 14.1 kN/m^2 is considered on the upper surface of the upper flange of each girder and an additional surface load of 17.1 kN/m^2 is applied to the end girders (1 and 5) due to the parapet.

Following the conclusions of previous studies [21, 22], live loads were not included in the analyses, since they do not have an appreciable influence on the fire response of the bridge.

4.6 Failure Assessment

The failure criteria proposed by Payá-Zaforteza and Garlock [21] were used, according to which the structure fails when the ultimate strain ε_u, is reached or when it becomes unstable. This can be identified as a rapid increment of the maximum vertical deflection, as a movement of a roller support towards the center of the span or as instability due to either lateral or web buckling.

5. Parametric study

This paper uses numerical models that combine CFD with FE to study the fire response of a typical steel girder bridge. To reach this goal the following parameters are studied: (a) the position of the fire load, (b) the elements included in the FE model (models including a single girder or the full bridge), (c) the restraint at the East support, (d) the vertical clearance of the bridge, (e) the general configuration of the bridge (one or three spans) and whether the bridge is supported on abutments or on two sets of piers. Table 1 gives the model parameters studied as well as a list of the analyses. The nomenclature is as follows:

- The first code specifies the fire scenario.
- The second code indicates if a single girder (code “SG”) or the full bridge (code “FB”) is analyzed with the FE model. In the former case, the number of the girder studied as defined in Fig. 1a is indicated after the code “SG”.
- The third code indicates the stiffness value of the horizontal spring (k_h) located at the East support, as explained in Section 4.3.
- The fourth code indicates the vertical clearance of the bridge expressed in m.

- The fifth code indicates if the bridge is a single span bridge supported on abutments (code “Ab”) or a three-span bridge with intermediate piers (code “Piers”).

The paper also includes a parametric study on the influence of the wind. Details of these analyses and a discussion of the results are given in Section 5.5.

All the FDS models were run as an MPI parallel job on a cluster made up of HP Proliant DL 580 servers (4 six-core AMD Opteron Model 8439 SE) under a Torque resource manager and scheduler. The resources assigned were 3 cores and 8 GB RAM per core. A typical simulation took 30 hours. All the thermal and structural models were run on a computer with a processor Intel Core i7-3632QM CPU @ 2.20GHz. A typical thermal analysis took 20 min. for a single girder bridge model and 90 min. for a full bridge model, while a typical structural analysis took 90 min. for a single girder and 20 hours for the full bridge. The results of the parametric study are given in the following subsections.

Please, cite this paper as: Peris-Sayol, G., Paya-Zaforteza, I., Alos-Moya, J., Hospitaler, A. Analysis of the influence of geometric, modeling and environmental parameters on the fire response of steel bridges subjected to realistic fire scenarios.Computers and Structures 2015,158:333-345. DOI: 10.1016/j.compstruc.2015.06.003

Table 1. Parameters and results of the analyses carried out.

Parametric Study	Analysis name	Position of the fire load	Size of the FE model	Girder	Horizontal restraint at the east support	Vertical clearance (m)	Bridge deck substructure	Failure				
								Time (min)	Mode[a]	Maximum deflection (m)	Maximum Transverse Displ. (m)	Cause
Horizontal stiffness at the east support	fire1-FB-k0-5-Ab	fire1	Full bridge	-	close to 0	5	Abutments	5.8	LB,S	0.72	0.1	LB
	fire1-FB-k∞-5-Ab	fire1	Full bridge	-	∞	5	Abutments	6.1	LB,S	1.02	0.19	LB
	fire2-FB-k0-5-Ab	fire2	Full bridge	-	close to 0	5	Abutments	3.9	WB,S	0.31	0.13	WB
	fire2-FB-k∞-5-Ab	fire2	Full bridge	-	∞	5	Abutments	3.2	LB,S	0.19	0.07	LB
Elements in the Structural Model - Full Bridge Vs Single Girder	fire1-SG1-k0-5-Ab	fire1	Single girder	1	close to 0	5	Abutments	19.6	WB,S	0.34	0.09	WB
	fire1-SG2-k0-5-Ab	fire1	Single girder	2	close to 0	5	Abutments	5.9	LB,WB,S	0.4	0.11	LB
	fire1-SG3-k0-5-Ab	fire1	Single girder	3	close to 0	5	Abutments	4.5	LB,S	0.35	0.08	LB
	fire2-SG1-k0-5-Ab	fire2	Single girder	1	close to 0	5	Abutments	5.9	WB,S	0.19	0.07	WB
	fire2-SG2-k0-5-Ab	fire2	Single girder	2	close to 0	5	Abutments	3.2	WB,S	0.24	0.09	WB
	fire2-SG3-k0-5-Ab	fire2	Single girder	3	close to 0	5	Abutments	3.0	WB,S	0.25	0.1	WB
Vertical clearance	fire1-SG3-k0-6-Ab	fire1	Single girder	3	close to 0	6	Abutments	5.5	LB,S	0.29	0.08	LB
	fire1-SG3-k0-7-Ab	fire1	Single girder	3	close to 0	7	Abutments	11.2	LB,S	0.19	0.1	LB
	fire1-SG3-k0-8-Ab	fire1	Single girder	3	close to 0	8	Abutments	27.7	LB,S	0.11	0.13	LB
	fire1-SG3-k0-9-Ab	fire1	Single girder	3	close to 0	9	Abutments	-	LB[b]	0.04	0.15	LB
	fire1-SG3-k0-10-Ab	fire1	Single girder	3	close to 0	10	Abutments	-	LB[b]	0.03	0.11	LB
	fire2-SG3-k0-6-Ab	fire2	Single girder	3	close to 0	6	Abutments	3.2	WB,S	0.26	0.11	WB
	fire2-SG3-k0-7-Ab	fire2	Single girder	3	close to 0	7	Abutments	3.4	WB,S	0.2	0.07	WB
	fire2-SG3-k0-8-Ab	fire2	Single girder	3	close to 0	8	Abutments	3.6	WB,S	0.21	0.07	WB
	fire2-SG3-k0-9-Ab	fire2	Single girder	3	close to 0	9	Abutments	4.3	WB,S	0.22	0.06	WB
	fire2 -SG3-k0-10-Ab	fire2	Single girder	3	close to 0	10	Abutments	5.3	WB,S	0.2	0.04	WB
Deck substructure	fire1-SG3-k0-5-Pier	fire1	Single girder	3	close to 0	5	Ab.+Piers	8.4	LB,S	0.19	0.1	LB
	fire2-SG3-k0-5-Pier	fire2	Single girder	3	close to 0	5	Ab.+Piers	3.88	WB,S	0.29	0.07	WB

[a] LB: Instability due to lateral buckling, S: Ultimate strain reached, WB: Instability due to web buckling in the contact with the abutment.

[b] In these models the structure does not collapse, altough significant out of plane displacements occur.

5.1 Horizontal restraint at the East support

Fig. 7 compares the evolution of the deflections of the most exposed girder of the bridge (Girder 3) obtained from the FE models of the full bridge for the fire scenarios and support conditions considered. The evolution of the maximum deflection of the bridge always follows a similar pattern and is described as follows:

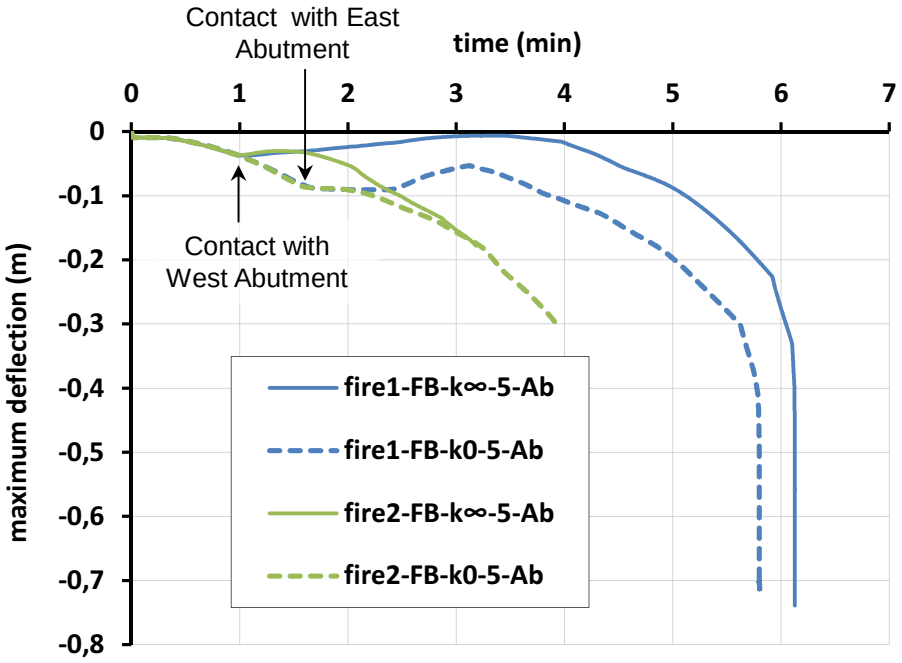

Fig. 7. Effect of the boundary condition (stiffness of the horizontal spring at the East support) on the evolution of the maximum deflection of Girder 3. Results obtained with FE models of the full bridge.

(a) First, the temperature increase of the bridge deck causes vertical deflections and makes it expand until the West sections (supported by the roller) contact the West abutment.

(b) The free expansion of the deck is now restrained, which introduces internal compression forces into the deck, with the following effects:

- In the models with k_h=∞: horizontal reaction forces at the hinged support that are likely to cause hinge failure.
- In the models with k_h close to 0: significant horizontal displacements in the East support. These displacements reach their maximum value (equal to the width of the expansion joint) when the end section of the bridge deck contacts the East abutment.

In both cases the restraint on horizontal displacement creates internal forces in the girders that tend to raise them until they lose stiffness due to the high temperature and finally yield. The deflections then increase until the bridge fails. Fig. 8a shows an example of the deformed bridge deck when it fails. The failure modes are as follows:

- In the models with k_h=∞ (see Fig. 8b) a local failure is observed at the vicinity of the hinged support (East Abutment) due to the compression forces caused by the deck contacting the West Abutment. In the "fire1" scenario considerable yielding is also observed at mid-span, where the bending moments are higher.

- In the models with k_h close to 0, yielding occurs in the girder web at the vicinity of the supports and in the mid-span region in the "fire1" scenario (see Fig. 8a). In "fire2", the yielding is concentrated directly above the blazing tanker in the vicinity of the East abutment and is followed by significant web buckling (see Figs. 8c and 8d).

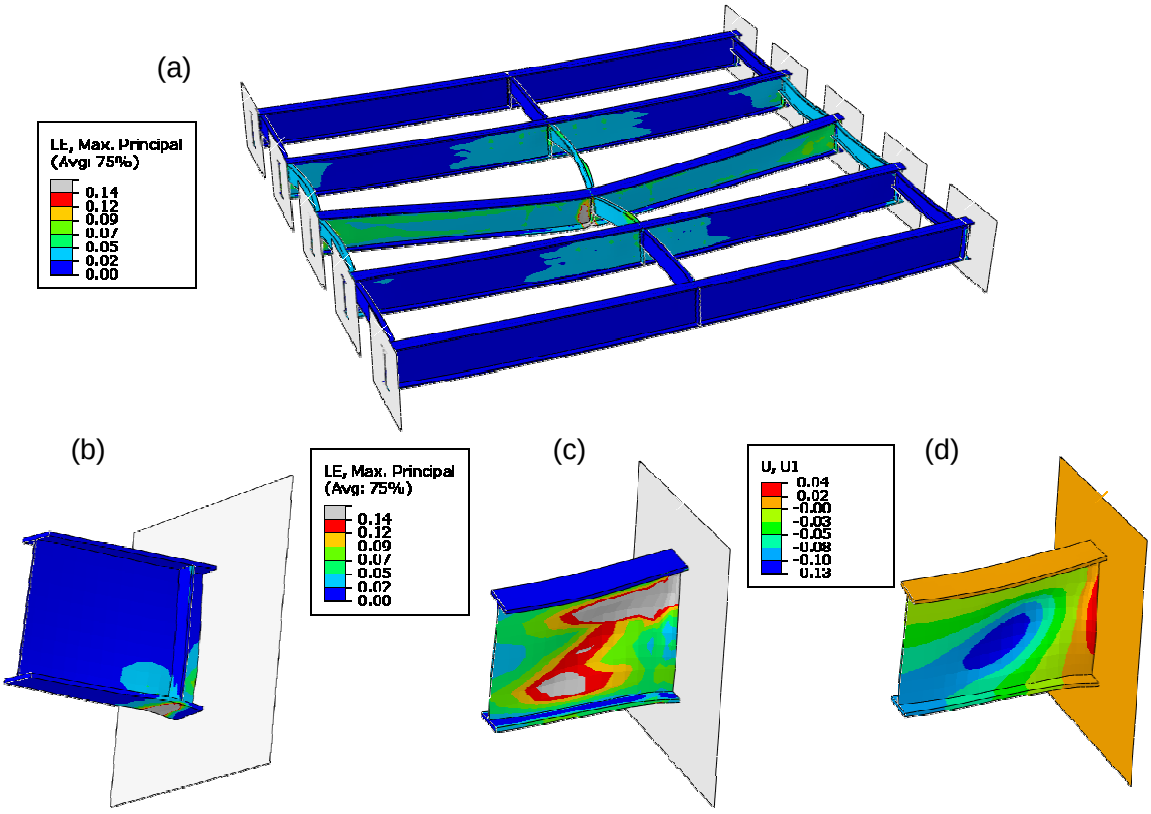

Fig. 8. Deformed shape of the bridge at failure according to the boundary condition used (a) Model fire1-FB-k0-5-Ab , deformed shape of the full bridge (b) Model fire2-FB-k∞-5-Ab . Local failure of Girder 3 near the pinned support. (c) Model fire2-FB-k0-5-Ab, yielding of Girder 3 near the East support, (d) Model Fire2-FB-k0-5-Ab, transverse (out-of-plane) displacements of Girder 3. Results obtained with FE models of full bridge. Grey areas in Figs. 8a, 8b and 8c correspond to yielded regions.

In all the cases analyzed, the failure of the bridge starts at Girder 3, which reaches the highest temperatures, and the "fire1" scenarios have the biggest deflections, as steel yielding appears in the supports and mid-span regions. It should be noted that times to failure are always smaller in the "fire2" scenarios, which have higher temperatures. Details on the times to failure and failure modes are given in Table 1.

The horizontal reaction at the East support is the important factor in deciding the horizontal restraint (k_h equal to ∞ or close to 0) at the pinned support to be considered in further analyses. This reaction is shown in Fig. 9 for the "fire1" scenario and a typical k_h=∞ model. The results show that once the deck contacts the West abutment, the girders suffer strong compression forces because the expansion of the bridge is limited by the hinged support and the abutment, which causes horizontal reactions at the hinged support. These reactions increase rapidly and reach a peak value between 2100 kN and 2300 kN, according to the fire scenario and girder considered. These forces are almost 30 times higher than the forces the bridge's pinned support has to withstand at ambient temperature due to the braking forces of passing vehicles (this braking force is close to be 80 kN/support, according to the AASHTO code [39]). The horizontal reaction forces caused by the fire are therefore likely to cause the hinged support to fail and would turn it into a roller or bearing with a very low capacity to restrain horizontal bridge displacements. As this hypothesis is for the case of the East support with horizontal spring stiffness close to 0, a value of k_h close to 0 is used in the remaining analyses in this paper.

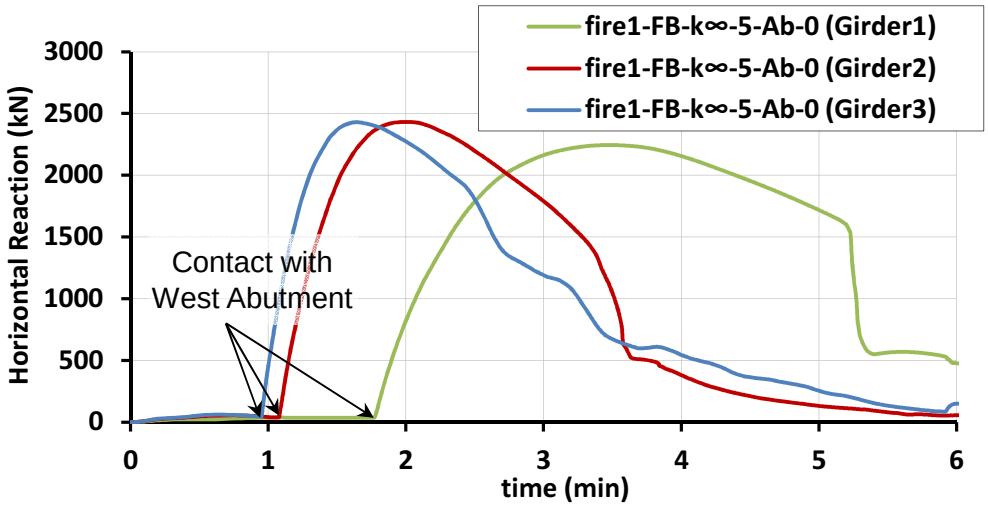

Fig. 9. Evolution of the horizontal reaction at the East support when a value of k_h=∞ corresponding to a hinge is considered. The FE model includes the full bridge.

5.2 Elements included in the FE model

Previous studies on the fire response of steel I-girder bridges [21, 22, 24] have analyzed a single girder, but not the full bridge. The goal of this simplification was to make FE models simpler and calculation times shorter, so that the FE models would be easier to build and more analyses could be done with less computational effort. This section assesses the validity of this simplification with additional FE thermo-mechanical models of each bridge girder and the results are compared to those provided by the FE analyses of the full bridge deck. Table 1 contains details of the analyses and their main results.

Fig. 10 compares the thermal results and shows the temperatures at four significant points in the cross section of the most exposed girders (2 and 3) for the "fire1" scenario in the steady state. The results obtained from the single girder and full bridge FE models are the same, as the corresponding temperature curves completely overlap (temperature differences are between 1 and 3ºC except in the areas of girder-transverse diaphragm contact, where they reach peak values of 10ºC). The same conclusion is obtained from the "fire2" scenario models. Therefore, as expected, no significant heat transfer occurs through the deck transverse diaphragms and concrete slab, so that from the thermal point of view, it is not necessary to build a FEM of the full bridge.

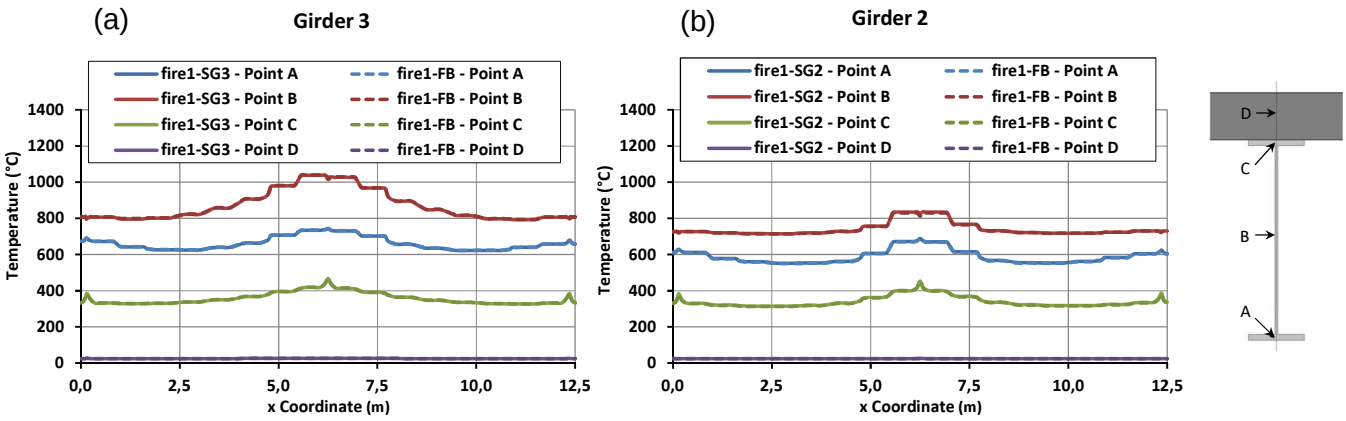

Fig. 10. "fire1" scenario. Temperatures in Girder 3 and Girder 2 in the steady state in thermal FE models including the full bridge or a single girder.

The influence of the size of the structural FE models is studied by comparing three types of result: i. e. deck deflections, times to failure and failure modes.

Please, cite this paper as: Peris-Sayol, G., Paya-Zaforteza, I., Alos-Moya, J., Hospitaler, A. Analysis of the influence of geometric, modeling and environmental parameters on the fire response of steel bridges subjected to realistic fire scenarios.Computers and Structures 2015,158:333-345. DOI: 10.1016/j.compstruc.2015.06.003

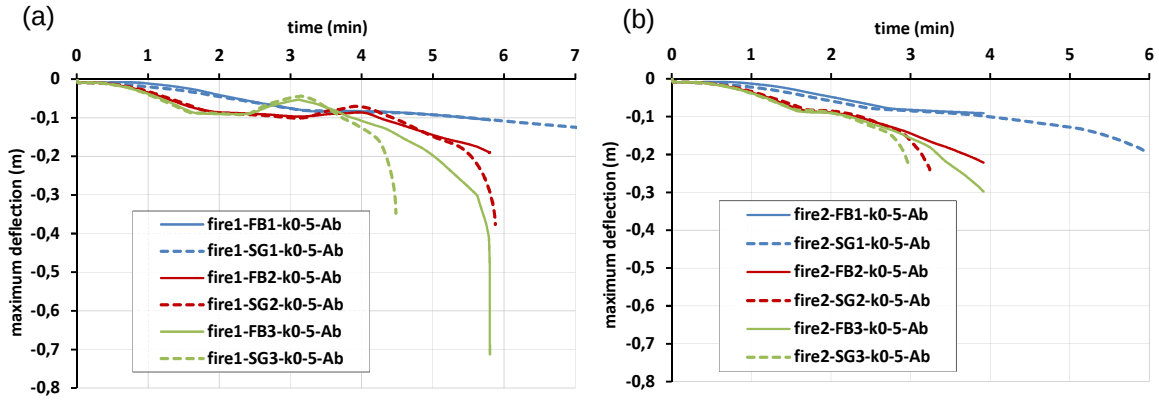

Fig. 11. Comparison of the evolution of the maximum deflections according to the size of the FE model: (a) “fire1” scenario, (b) “fire2” scenario.

Fig. 11 shows the evolution of the maximum deflections of each bridge girder and type of FE model used for both fire scenarios. The structural behavior is very similar until significant yielding or until the first plastic hinge develops in Girder 3. When this happens:

- Girder 3 experiences runaway and fails in the FE models containing a single girder.

- In the full bridge models Girder 3 transfers part of the load to the rest of the deck through the transverse diaphragms, which causes longer times to failure and greater maximum deflections. This process continues until additional significant yielding occurs and the structure fails. Note that when this happens, the structural analysis of the full bridge stops, even if Girder 1 still keeps its load-bearing capacity. This means Girder 1 has longer times to failure in the single girder than in the full bridge analysis.

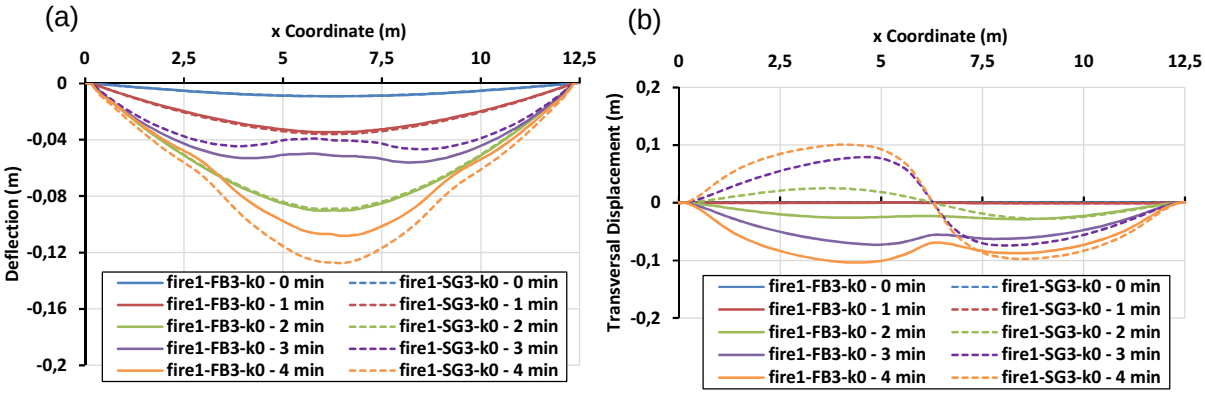

Fig. 12. Comparison of vertical deflections and transverse displacements in Girder 3 for the “fire1” scenario according to the FE models used (full bridge versus single girder).

Fig. 12a and 12b show, respectively, the evolution of the deflections of Girder 3 as well as the transverse (out-of-plane) displacements of the central bottom fiber of Girder 3's bottom flange in the "fire1" scenario, according to the elements included in the FEM. The following comments are relevant:

- The evolution of the deflections is very similar in all cases. There is a difference of 2 cm in maximum deflection, which is not important from the engineering point of view. This difference is explained by the presence of transverse diaphragms in the FEM that make it possible for all the girders to combine in resisting the applied loads. Similarly, when Girder 3 experiences an upward movement, the transverse diaphragms tie Girder 3 to the adjacent girders, this results in smaller lifting movements in the full bridge model. Time to failure of Girder 3 is 4.5 min, which is less than the 5.8 min needed by the full bridge model to reach the collapse of the structure. From the engineering point of view the difference is not important because the time at which significant yielding appears is the same (around 3.2 min after the start of the fire) and is probably the most critical time, as it marks the point at which significant rehabilitation work or even replacement of the deck will be required.

- The failure mode (instability due to lateral buckling) is the same, but the buckling mode shapes differ. In the single girder model, transverse diaphragms are not included in the FE model, but their influence is considered by imposing null out-of-plane displacements at the intersection of Girder 3 with the diaphragms. These conditions mean the buckling length of the beam is half of the span-length (as there are transverse diaphragms at the supports and at mid-span sections). However, as the transverse diaphragms do not have infinite axial stiffness, when the FEM includes the full bridge, the diaphragms do not completely prevent the out-of-plane displacements in Girder 3, which gives the buckling mode shown in Fig. 12b.

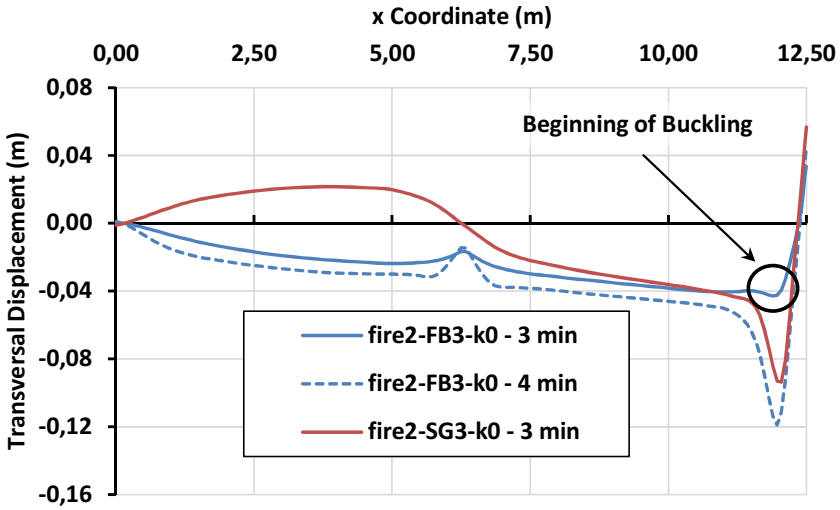

Fig. 13. "fire2" scenario. Transverse (out of plane) displacement of Girder 3's mid-web according to the size of the FE model.

Fig. 13 shows the transverse out-of-plane displacements of Girder 3's mid-web in the "fire2" scenario. The results show that the failure mode, which is due to web buckling in the vicinity of the East support, does not depend on the type of model considered (full bridge or single girder). The evolution of the deflections and the times to failure follow the same pattern as in the "fire1" scenario and its analysis is not repeated. Mid-web temperatures at failure are around 950-1100ºC for both fire scenarios.

Summarizing: single girder models reproduce the same failure modes as full bridge models, have similar critical temperatures and provide reasonably conservative predictions of the time to failure. Single-girder models will therefore be used in the rest of the parametric study. This decision is also supported by the fact that single girder models require much shorter calculation times than full bridge models (up to 4.5 times less for thermal models and 13 times less for structural models).

5.3 Vertical clearance of the bridge.

This section analyzes the influence of the vertical clearance of the bridge on its fire response, for which ten further analyses were carried out (see Table 1) to have results related to clearances between 5 and 10 m. Fig. 14 shows the maximum adiabatic temperatures at the most thermally exposed section of the bridge in the steady state, as well as the analytical relations between the vertical clearance (v) and adiabatic temperatures (T). The different times to failure and failure modes can be seen in Table 1.

The following conclusions can be drawn from the results:

- As expected, temperatures decrease as vertical clearance increases (see Fig. 15a and b), because the greater the clearance the smaller the surface of the bridge affected by the flames. The maximum temperature values of the temperature drop is close to 720 ºC for "fire1"· scenarios and close to 250 ºC for "fire2". The effect of the temperature drop is much more noticeable in Fire1 due to the Coandă effect [40], or the tendency of a jet of fluid to be attracted to a nearby surface. In the "fire2" scenario, the Coandă effect causes the flames to adhere to the walls of the East Abutment and reach higher levels (see Fig. 15c), which results in further heating of the bridge deck.

- Vertical clearance influences the time to failure but does not change the failure mode. As the clearance increases, the temperatures in the bridge decrease and time to failure gets longer. For example, they are 22% and 520% for "fire1" scenarios and 6% and 22% for "fire2", when clearance is increased from 5 m to 6 m and 8 m respectively. Fig. 16 details the evolution of the maximum vertical deflection of Girder 3. It is noticeable that the failure modes are not influenced by the clearance, as neither the overall shape of all the deflection curves (see Fig. 16) nor the girder region with the highest temperature depends on this factor. Also noteworthy is the fact that in "fire1" scenarios the bridge has not collapsed one hour after the start of the fire when clearance is equal to or greater than 9 m.

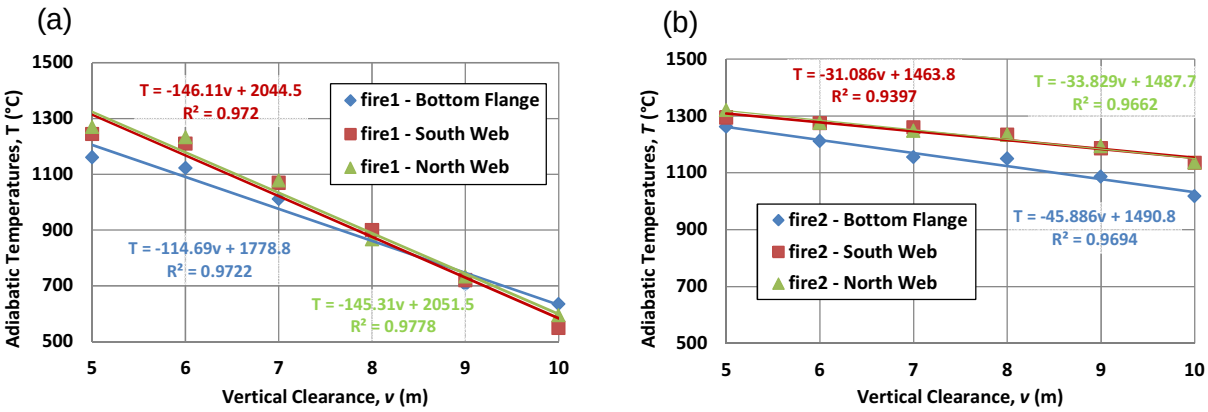

Fig. 14. Influence of vertical clearance on the steady state adiabatic temperatures in the most thermally exposed section of the bridge: (a) mid-span section of Girder 3 for the "fire1" scenario, (b) section of Girder 3 close to the East Abutment for the "fire2" scenario.

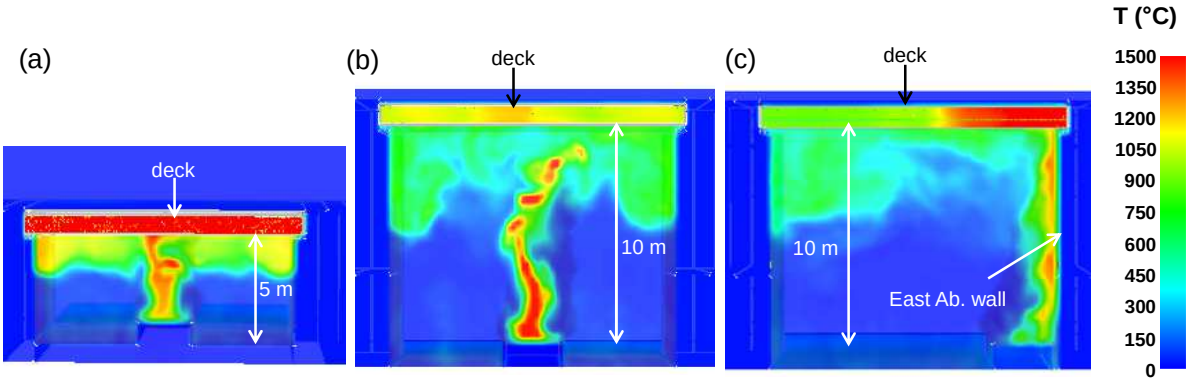

Fig. 15. Longitudinal section of the bridge for Girder 3 showing FDS temperature results at the steady state: (a) “fire1” scenario, 5 m clearance, (b) “fire1” scenario, 10 m clearance, (c) “fire2” scenario, 10 m clearance.

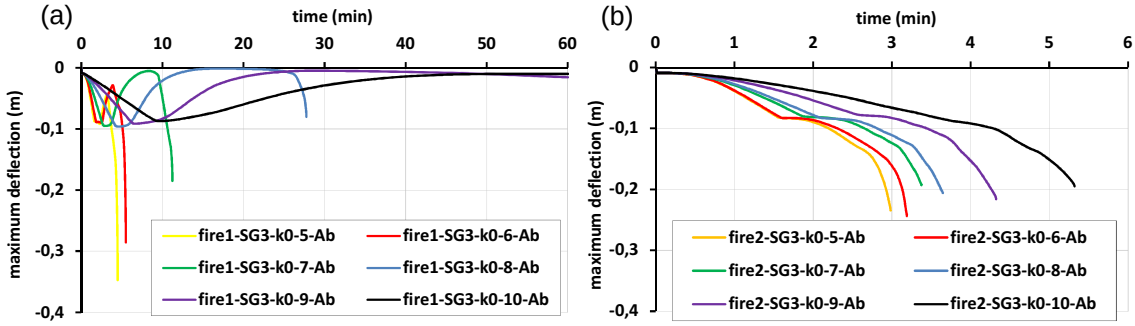

Fig. 16. Influence of vertical clearance on the maximum vertical deflection of Girder 3: (a) “fire1” scenario, (b) “fire2” scenario.

5.4 General configuration of the bridge and deck substructure

In this section, the influence of the general configuration of the bridge and deck substructure is studied by comparing the fire response of the reference case study (a simply supported single-span bridge supported on two full-retaining U-shaped abutments) to the response of a three-span bridge with the same span length as the reference case study, with the fire load under the central span and the central span supported on two sets of piers. Fig. 17 shows a general view of the three-span bridge in the steady state of a “fire2” scenario. Table 1 and Figs. 18 and 19 detail the main results obtained.

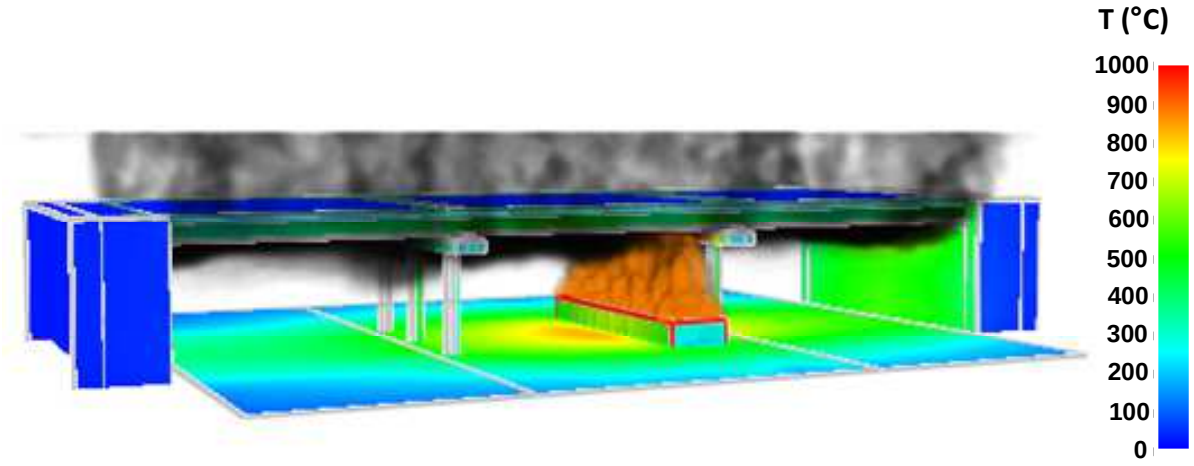

Fig. 17. General view of three-span bridge in the steady state of the "fire2" scenario showing the temperatures obtained with FDS.

The results show that times to failure increase from 4.5 min ("fire1") and 3 min ("fire2") in the case study to 8.5 min ("fire1") and 4 min. ("fire2") in the three-span bridge, which represents an increase in time to failure of 89% and 33%, respectively. This increase is due to the lower temperatures reached by the bridge deck when supported on piers, because: (a) better ventilation of the area where the fire takes places results in less accumulation of heated gas around the bridge deck, and (b) the Coandă effect, which plays a major role in the "fire2" scenarios, is now less important. The maximum temperature decrease reaches values close to 250ºC ("fire1") and 340ºC ("fire2") in the areas furthest away from the burning tanker and is much smaller immediately above it (see Fig. 18). This explains the bigger increase of time to failure in the "fire1" scenario, as the failure in this case is caused in great part by the yielding of the steel in the area close to the abutments, where the temperature decrease is maximum. That the failure modes do not depend on the general configuration of the bridge is proved by the fact that the overall shape of the curves showing the evolution of the maximum bridge deflections (see Fig. 18) does not change. Web temperatures in the hottest section at the time of collapse vary between 970 and 1165 ºC.

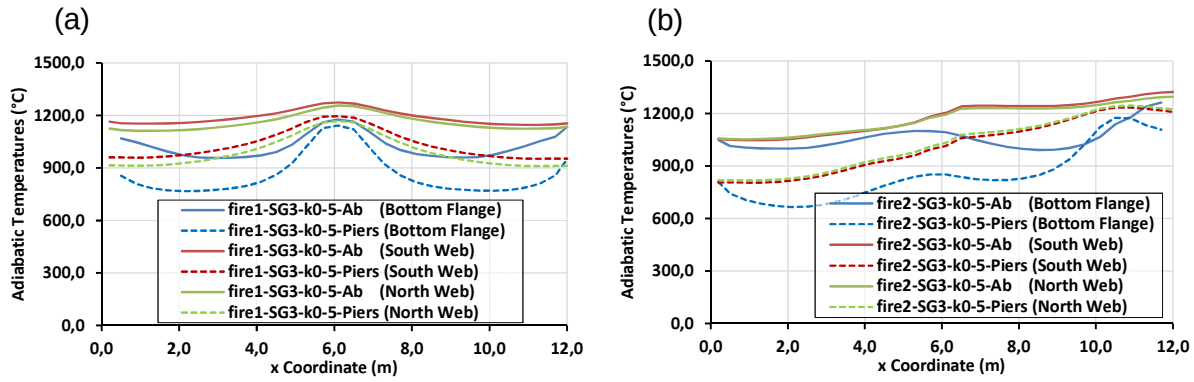

Fig. 18. Influence of the number of bridge spans on the adiabatic temperatures of Girder 3: (a) "fire1" scenario, (b) "fire2" scenario.

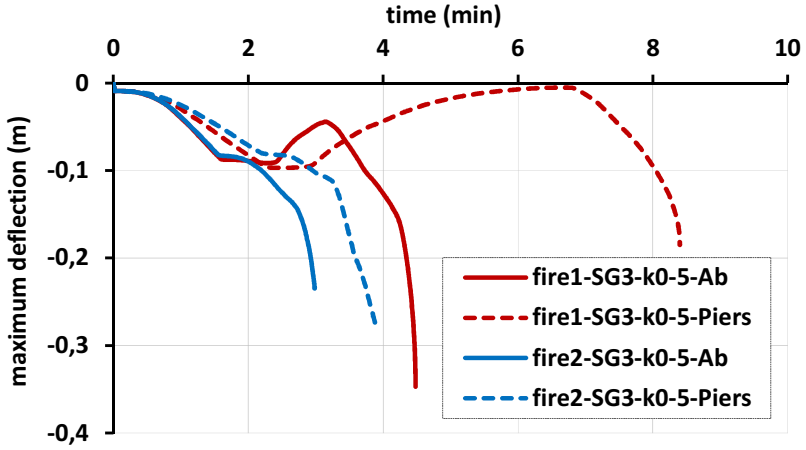

Fig. 19. Influence of the number of bridge spans on the maximum vertical deflection of Girder 3.

5.5 Wind

Finally, the influence of wind was considered by studying the fire response in the case study to six different wind speeds (0, 1, 4, 8, 12, and 16 m/s) at the time of the tanker accident, with the wind blowing perpendicular to the longitudinal axis of the bridge. Fig. 20a shows Girder 3's adiabatic temperatures in the steady state for the "fire1" scenario. The results show that the wind blows the flames away from the bridge (Fig. 20b), thus reducing bridge temperatures. Therefore, in cases of tanker fires under a bridge it is conservative not to consider any wind in the analyses. However, it should also be pointed out that, in fires where the tanker is outside of the bridge's footprint, the wind could blow the flames towards the bridge and produce some damage, although an accident with the tanker fire under the bridge would always be worst. Results are similar for the "fire2" scenario and for the sake of brevity are not plotted in Fig. 20.

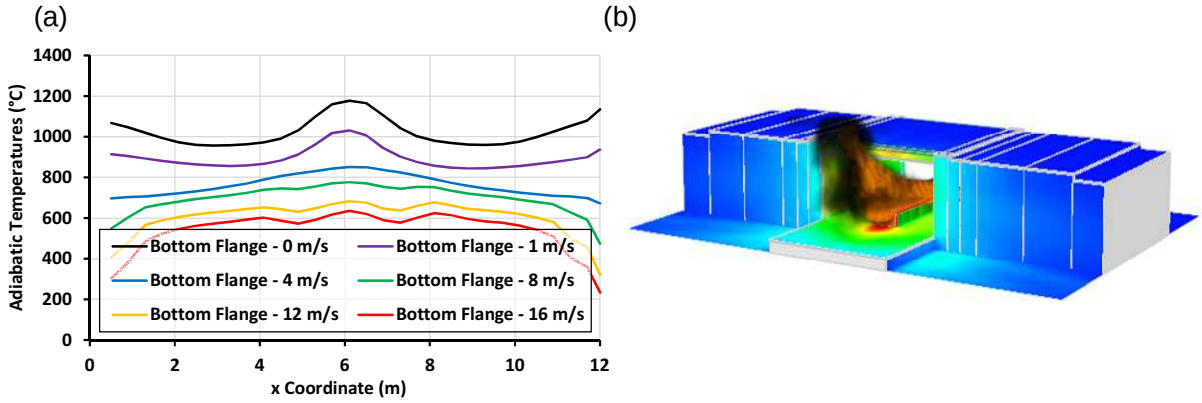

Fig. 20. Influence of the presence of wind perpendicular to the bridge longitudinal axis in "fire1" scenario: (a) adiabatic temperatures in the bottom flange of Girder 3 according to wind speed, (b) 3D view of bridge showing the wind effect on flames when the wind speed is 8 m/s.

6. Conclusions and future work

Bridge fires are currently a major concern due to the high number of such events and the damage they can cause. Despite this, building codes do not detail how to deal with bridge fires and little research has been carried out on the topic. This paper proposes guidelines for the numerical modeling of simply-supported steel girder bridges and studies the influence of geometrical and environmental parameters on their fire response. The following conclusions can be drawn from the set of analyses carried out:

- The heating of the bridge causes very high horizontal reaction forces in the bridge deck hinges. These forces are very likely to cause hinge failure and reduce their capacity to restrain horizontal deck movement. The hinges should therefore be modeled in the structural simulations as rollers with horizontal spring stiffness close to 0.

- The fire response of the bridge deck can be obtained with FE models of the most exposed girder and does not require building a model of the full bridge deck. This is possible because, when appropriate boundary conditions are used, single girder FE models: (a) reproduce the same failure modes and have critical temperatures similar to those obtained with full bridge models, (b) provide reasonable conservative predictions of the bridge times to failure. The simplification of using single girder instead of full bridge deck models is important, as it enables considerable modeling and calculation time savings.

- Fire scenarios with the burning tanker close to an abutment are more unfavorable than under the mid-span because they result in higher temperatures due to the Coandă effect and shorter times to failure.

- Increasing the bridge vertical clearance reduces the damage caused by a fire under the bridge. This effect is more marked for scenarios involving a tanker under the bridge mid-span. The relation between vertical clearance and temperatures in the most exposed section of the bride is linear.

- Multi-span bridges have a better fire response than single-span bridges supported by full-retaining abutments because of the better ventilation of the fire affected area and the lesser importance of the Coandă effect in the case of multi-span bridges.

- The presence of wind generally reduces the effects of fires, although it can also blow a fire towards a bridge if it starts outside the bridge footprint.

The research presented in this paper focuses on the study of existing steel I-girder bridges where the concrete slab is not structurally connected to the girders. Future research should include composite bridges, as this structural system is commonly used nowadays for bridges with span lengths similar to the one analyzed in this paper.

Acknowledgements.

Funding for this research was provided by the Spanish Ministry of Science and Innovation (Research Project BIA 2011–27104) and the Universitat Politècnica de València (Research and Development Support Program PAID-06-11). All opinions expressed in this paper are the authors' and do not necessarily reflect the policies and views of the sponsors.

References

[1] Chang S and Nojima N. Measuring post-disaster transportation system performance: the 1995 Kobe earthquake in comparative perspective. Transportation Research Part A 2001; 35: 475–484.

[2] Zhu S., Levinson D, Liu HX, Harder K. The traffic and behavioral effects of the I-35W Mississippi River bridge collapse . Transportation Research Part A: Policy and Practice 2010 44 (10): 771-784.

[3] Ghosn M, Moses F, Wang J. NCHRP Report 489. Design of Highway Bridges for Extreme Events. Transportation Research Board of the National Academies. Washington D.C., USA. 2003.

[4] Cheng J. Reliability analysis of the Sutong Bridge Tower under ship impact loading, Structure and Infraestructure, doi: 10.1080/15732479.2012.757792

[5] Mostafaei H and McCartney C. Vulnerability of bridges and other critical infrastructure to extreme fire and BLEVEs. NRC research Report nº 4259. 2012. [68 pages].

[6] Wright W, Lattimer B, Woodworth M, Nahid M, Sotelino E. Highway Bridge Fire Assessment Draft Final Report. Prepared for the NCHRP Program Transportation Research Board of the National Academies. Virginia Polytechnic Institute and State University, 2013. [492 pages].

[7] San Francisco Gate. The Maze Meltdown. www.sfgate.com [Accessed August 30, 2014].

[8] Chung P., Wolfe R.W., Ostrom T., Hida S. Editors. Accelerated Bridge Construction Applications in California- A “Lessons Learned”. Report issued by the California Department of Transportation, 2008. [55 pages].

[9] PennLive. No. 8 - Catastrophe on I-81 overpass is a $13 million wake-up call: 13 for '13. www.pennlive.com [Accessed August 30, 2014].

[10] Garlock ME, Paya-Zaforteza I, Gu L, Kodur V. Fire Hazard in Bridges: Review, Assesment and Repair Strategies. Engineering Structures 2012;35:89–98.

[11] Mostafaei H, Sultan M, Kashef A. Resilience assessment of critical infrastructure against extreme fires. In Proc. of the 8th International Conference on Structures in Fire. Shanghai, China, June 12-13, 2014, p. 1153-1160.

[12] Jiang J, Usmani A. Modeling of steel frame structures in fire using OpenSees. Computers & Structures 2013; 118:90-99.

[13] Couto C, Vila Real P, Lopes N, Rodrigues JP. Buckling analysis of braced and unbraced steel frames exposed to fire. Engineering Structures 2013; 49: 541-59.

[14] Quiel SE, Garlock MEM, Paya-Zaforteza I. Closed Form Procedure for Predicting the Capacity and Demand of Steel Beam-Columns under Fire. ASCE Journal of Structural Engineering 2011; 137: 967-76.

[15] Moura Correia AJP, Rodrigues JPC, Gomes FCT. A simplified calculation method for fire design of steel columns with restrained thermal elongation. Computers & Structures 2013; 116: 20-34.

[16] Moliner V, Espinos A, Romero ML, Hospitaler A. Fire behavior of eccentrically loaded slender high strength concrete-filled tubular columns. Journal of Constructional Steel Research 2013; 83:137-146.

[17] Xi F, Li QM, Tan YH. Dynamic response and critical temperature of a steel beam subjected to fire and subsequent impulsive loading. Computers & Structures 2014; 135: 100-108.

[18] Elhami Khorasani N, Garlock M, Gardoni P. Fire load: Survey data, recent standards, and probabilistic models for office buildings. Engineering Structures 2014; 58: 152-165.

[19] Wang Y, Dong Y, Zhou G. Nonlinear numerical modeling of two-way reinforced concrete slabs subjected to fire. Computers & Structures 2013: 23-36.

[20] C. Maraveas and A.A. Vrakas. Design of Concrete Tunnel Linings for Fire Safety. Structural Engineering International 2014; 24: 319-329, doi: 10.2749/101686614X13830790993041

[21] Payá-Zaforteza I, Garlock M. A numerical investigation on the fire response of a steel girder bridge. Journal of Constructional Steel Research 2012; 75: 93-103.

[22] Alos-Moya J, Paya-Zaforteza I, Garlock M.E.M., Loma-Ossorio E, Schiffner D, Hospitaler A. Analysis of a bridge failure due to fire using computational fluid dynamics and finite element models. Engineering Structures 2014; 68: 96-110.

[23] Chen W, Duan L. Bridge Engineering Handbook. New York, 2000.

[24] Aziz E.M., Kodur V.K., Glassman J.D. and Garlock M.E. Moreyra. Behavior of steel bridge girders under fire conditions. Journal of Constructional Steel Research 2015; 106: 11-22.

[25] Quiel SE, Yokoyama T, Bregman L.S., Mueller K.A., Marjanishvili S.M. A streamlined framework for calculating the response of steel-supported bridges to open-air tanker truck fires. Fire Safety Journal 2015; 73: 63-75.

[26] Gong X., Agrawal A.K. Numerical simulation of fire damage to a long-span truss bridge. Journal of Bridge Engineering 2014; doi: 10.1061/(ASCE)BE.1943-5592.0000707

[27] Xanthakos TE. Theory and design of bridges. New York, USA : John Wiley and Sons, 1994.

[28] Mc Grattan K, McDermott R, Hostikka S, Floyd J. Fire Dynamics Simulator (version 5). User's Guide. NIST Special Publication 1019-5, Gaithersburg, MD, USA, 2010.

[29] Simulia. Abaqus/standard version 6.9 user's manual; 2009.

[30] Mc Grattan K, Hostikka S, Floyd J, Baum H,Rehm R, Mell W, McDermott. Fire Dynamics Simulator (Version 5). Technical Reference Guide. Volume 1: Mathematical model. NIST Special Publication 1018-5, Gaithersburg, MD, USA, 2010.

[31] Peris-Sayol G, Alós-Moya J, Payá-Zaforteza I, Hospitaler-Pérez A. Estudio paramétrico de la respuesta termo-estructural de un puente metálico multijácena sometido a incendios reales. A parametric study on the thermo-mechanical response of a multi-girder steel bridge submitted to real fires. *Informes de la Construcción* 2014; 66(Extra-1): m002 doi: 10.3989/ic.13.077. In Spanish.

[32] Society of Fire Protection Engineers. *SFPE Handbook of Fire Protection Engineering*. 3th Edition. NFPA, USA; 2002. ISBN 087765-451-4.

[33] Wickstrom U, Dat Duthinh D, McGrattan K. Adiabatic Surface Temperature for Calculating Heat Transfer to Fire Exposed Structures. Interflam 2007. September 2007, Vol. 2: 943-953.

[34] Peris-Sayol G, Payá-Zaforteza I, Alós-Moya J, Hospitaler A. Análisis de la influencia del tipo de elemento finito empleado en la respuesta frente al fuego de un puente metálico. Influence of the finite element model used in the fire response of a steel bridge. In Proc. of the Third Fire Engineering Conference. Valencia, Spain, October 23rd, 2014. In Spanish.

[35] European Committee for Standardization (CEN). EN 1992-1-2:2011 Eurocode 2. Design of concrete structures, Part 1-2: General rules - Structural fire design, European Committee for Standardization. Brussels, Belgium. 2011.

[36] European Committee for Standardization (CEN). EN 1993-1-2:2011 Eurocode 3. Design of steel structures, Part 1-2: General rules - Structural fire design, European Committee for Standardization. Brussels, Belgium. 2011.

[37] Peris-Sayol G, Payá-Zaforteza I, Alós-Moya J. Analysis of the response of a steel girder bridge to different tanker fires depending on its structural boundary conditions. In Proc. of the 8th International Conference on Structures in Fire. Shanghai, China, June 12-13, 2014.

[38] European Committee for Standardization (CEN). Eurocode 1 Actions on structures, part 1–2: general actions – actions on structures exposed to fire. Brussels (Belgium): CEN; 2002.

[39] American Association of State Highway and Transportation Officials (AASHTO). LRFD Bridge design specifications. Washington D.C, USA; 2012.

[40] Faber TE. Fluid Dynamics for Physicists. Cambridge, UK : Cambridge University Press, 1995.